Ionic Strength Effect Alters the Heterogeneous Ozone Oxidation of Methoxyphenols in Going from Cloud Droplets to Aerosol Deliquescent Particles

Ionic strength effect alters the heterogeneous ozone oxidation of methoxyphenols in going from cloud droplets to aerosol deliquescent particles

Majda Mekic[1,2], Yiqun Wang[1,2], Gwendal Loisel[1], Davide Vione[3], Sasho Gligorovski[1*]

[1]State Key Laboratory of Organic Geochemistry, Guangzhou Institute of Geochemistry, Chinese Academy of Sciences, Guangzhou 510 640, China

[2]University of Chinese Academy of Sciences, Beijing, China

[3]Dipartimento di Chimica, Università degli Studi di Torino, Via Pietro Giuria 5, 10125 Torino, Italy

Submitted to *Environmental Science & Technology*

* Correspondance to:
Sasho Gligorovski
gligorovski@gig.ac.cn

Abstract

Methoxyphenols represent one of the most abundant classes of biomarker tracers for atmospheric wood smoke pollution. The reactions of atmospheric oxidants (ozone, OH) with methoxyphenols can contribute to the formation of secondary organic aerosols (SOA). Here for the first time we use the well-established vertical wetted wall flow tube (VWWFT) reactor to assess the effect of ionic strength (I), pH, temperature, and ozone concentration on the reaction kinetics of ozone with acetosyringone (ACS), as a representative methoxyphenol compound. At fixed pH = 3, typical for acidic atmospheric deliquescent particles, and at I = 0.9 M adjusted by Na_2SO_4, the uptake coefficient (γ) of O_3 increases by two orders of magnitude from $\gamma = (5.0 \pm 0.8)\times10^{-8}$ on neat salt solution (Na_2SO_4) to $\gamma = (6.0 \pm 0.01) \times10^{-6}$ on a mixture of ACS and Na_2SO_4. The comparison of the uptake coefficients of O_3 at different pH values indicates that the reaction kinetics strongly depends on the acidity of the phenolic group of ACS. The observed different reactivity of gas-phase ozone with ACS has implications for its uptake by the dilute aqueous phase of cloud droplets and by aerosol deliquescent particles loaded with inorganic salts, and can affect the formation of SOA in the atmosphere.

1 Introduction

Combustion processes release myriad of compounds into the atmosphere while ozone (O_3) is formed through secondary chemistry.[1] Modeling study has estimated that pyrogenic emissions from biomass burning (BB) contribute around 10% to the total tropospheric ozone concentration on the global scale.[2] BB, which is becoming a global concern,[3] is also a significant source of smoke particulate matter (PM).[4] Mazzoleni et al. (2007)[5] reported that BB is an important source of 4-substituted methoxylated phenolic compounds (methoxyphenols), which were detected in substantial amounts and were classified as dominant organics found in most of the ambient samples. Methoxylated phenols could also be formed as photolysis products of polycyclic aromatic hydrocarbons (PAHs), which are also emitted in high quantity during BB, as suggested by Vione et al. (2006)[6] and references therein. Methoxyphenols are among the most abundant, widely spread and, as a consequence, most exploited biomarker tracers for atmospheric wood smoke pollution.[3,7] They are classified as semi-volatile polar organic molecules with low molecular masses, which could be distributed in both, gas-phase and particulate-phase.[5,8] According to the field measurements, acetosyringone (ACS) is a major contributor to the particle-phase emissions from oak and eucalyptus wood combustion, with emission rates of 28.1 and 55.3 mg kg^{-1} of burned wood, respectively.[9] The kinetics and reaction mechanisms of gas phase and heterogeneous reactions of methoxyphenols with atmospherically relevant oxidants, O_3, hydroxyl radicals (OH), and nitrogen dioxide (NO_2), have been previously studied.[10-17.]

It has been reported that heterogeneous oxidation reactions can cause significant chemical modifications of phenolic constituents.[18-21] Moreover, few studies concluded that gas-phase reactions of OH with methoxyphenols are potentially important sources of SOA.[22-24]

Ozone is an important atmospheric oxidant, the mixing ratios of which have shown an increasing trend over the last years.[25-29] Ozone mixing ratios over 200 ppb have been regularly detected during pollution events, which may be a serious human health concern.[26,30] The ionic strength (I) in the dilute aqueous phase of cloud droplets, which ranges between 7.5×10^{-5} and 7.5×10^{-4} mol L^{-1}, is quite different compared to that in aerosol deliquescent particles that are loaded with inorganic salts.[31] The ionic strength in marine aerosols can reach values of up to 6 mol L^{-1}, while in the urban aerosols it can be as high as 18.6 mol L^{-1}.[32] Severe haze events contain aerosol deliquescent particles with ionic strength levels of up to 43 mol L^{-1}.[33]

For this reason, the chemical transformation processes of organic compounds in cloud droplets can differ substantially from those in aerosol deliquescent particles. However, our understanding of the ionic strength effect on oxidation processes in aerosol deliquescent particles lags substantially behind that for the dilute aqueous phase.

In this study, we use a vertical wetted wall flow tube (VWWFT) reactor to assess the influence of ionic strength on heterogeneous reactions of gaseous O_3 with liquid films consisting of ACS. The effect of temperature and pH on the uptakes of O_3 on aqueous ACS was evaluated, as well. Our findings suggest that methoxyphenols released into the atmosphere from various sources might be a significant sink of tropospheric ozone, through heterogeneous reaction with aerosol particles in the presence of high ionic strength.

2 Experimental

2.1 Experimental set-up

The VWWFT methodology was utilized to determine the heterogeneous reaction between gas-phase ozone and the aqueous layer. The latter consisted of neat ACS or a mixture of ACS and different concentrations of Na_2SO_4, under controlled conditions. The experimental set-up has been previously described in detail.[34] Briefly, the reactor is an 80-cm long, vertically-aligned cylinder made up of borosilicate glass, with a diameter (d) = 0.9 cm. The flow tube was thermostated by water circulation (Lauda, RC Germany), and the temperature was varied between 278.15 K and 318.15 K (± 0.02 K). The freshly prepared solution was pumped (5 mL min^{-1}) by peristaltic pump (LabV1/MC4, SHENCHEN, China) into the top of the reactor. Then, the homogenous thin liquid film flowed downwards into the inner flow tube, under the influence of gravity. As a result, no ripples were detected and a laminar flow of the liquid film was established with Reynolds number lower than 10 (Re = 0.2). Gaseous ozone was generated by photolysis of a flow of pure oxygen (O_2) (purity 99.999%, Guangzhou Kehanda Trading, China). The oxygen flow (200 mL min^{-1}, measured with Sevenstar CS200) passed through a commercial ozone generator (UVP, LLC Upland), and the obtained ozone was introduced into the flow tube from the top of the reactor by means of a movable glass injector. Both the gas-phase ozone and the liquid film flowed downwards the flow tube in parallel, with the same flow rate (5 mL min^{-1}). As a result, the length of the exposed aqueous solution could be varied by moving the glass injector. The flow of ozone at the exit of the flow tube reactor was diluted with air (purity of 99.999%, Guangzhou Kehanda Trading, China; flow rate of 1300 mL min^{-1}, Sevenstar CS200) prior to the monitoring of O_3 by the ozone analyzer (Thermo Scientific Model 49i, USA).

Aqueous solutions of ACS ([ACS] = 1×10^{-6} mol L^{-1}) (Sigma-Aldrich, 98.5%) or mixtures of ACS and Na_2SO_4 (0 mol L^{-1} < I (ionic strength) < 0.9 mol L^{-1}) (Sigma Aldrich, ≥ 99.0%) were prepared with ultra-pure water (Sartorius 18 MΩ, H_2O-MM-UV-T, Germany). Using a pH meter (Thermo Scientific), the various pH values of the ACS solutions were adjusted between pH 3 and 10 by drop-wise addition of a prepared 1 mol L^{-1} solution of HCl or NaOH.

For the modeling of the uptake coefficient, a non-linear data fit was carried out with the FigP software (Biosoft, UK), equipped with the P.Fit equation fitting engine.

2.2 Data analysis

The loss of gas-phase ozone upon heterogeneous reactions is described by its uptake coefficient (γ), which is defined as the probability that a collision between gas-phase molecules of O_3 and the liquid surface (*i.e.*, an aqueous solution of ACS or a mixture of ACS and Na_2SO_4) leads to the net uptake of O_3 into the condensed phase.[21,35]

$$\gamma = \frac{number\ of\ lost\ molecules}{number\ of\ colliding\ molecules} \quad \text{(Eq-1)}$$

The effective loss of gas-phase ozone is described with the following law:

$$\ln\left(\frac{[O_3]_t}{[O_3]_0}\right) = -k_{1st} \cdot t \quad \text{(Eq-2)}$$

where ($[O_3]_t/[O_3]_0$) is the ratio of ozone concentration at time *t vs.* initial ozone concentration, k_{1st} is the pseudo first-order rate constant for the reaction of gaseous ozone with the liquid film (consisting of either ACS, or a mixture of ACS/Na_2SO_4), and *t* is the residence time of ozone in the reactor. Figure S1 shows the plot of ($[O_3]_t/[O_3]_0$) *versus* the residence time of O_3 in the

reactor. The slope of the plot depicted in Figure S1 gives the value of k_{1st} according to Eq-2, which is needed to estimate the reactive uptake coefficients of O_3 (Eq-4, *vide infra*).

It is considered that the mass accommodation coefficient (α) >> γ because the uptake coefficient of O_3 measured on the liquid film of ACS was relatively low (10^{-6}-10^{-7}).[36,37] The uptake coefficient of O_3 depends on the solubility of ozone in the aqueous solution, i.e. the Henry's law constant, H_{O3}, and the diffusion coefficient of O_3, D_{O3}, in the aqueous phase.[17,34,36-38]

In the case of a slow aqueous phase reaction, liquid-phase diffusion processes would not affect the uptake coefficient of ozone because the liquid-phase reactions are not fast enough to compete with the diffusion of O_3 into the solution;[36,37] hence, the diffusion process is not the rate-determining step. On these assumptions, one obtains the first-order rate of O_3 loss from the gas phase as follows:[38]

$$\frac{d[O_3^g]}{dt} = \gamma \frac{\bar{v}}{2r}[O_3^g] = k_{2nd}[ACS][O_3^g]H_{O3} = k_{2nd}[ACS][O_3^{aq}] \quad \text{(Eq-3)}$$

In Eq-3, $[O_3^g]$ and $[O_3^{aq}]$ are ozone concentrations in gas and liquid phase, respectively, $\bar{v}$ is the mean thermal molecular velocity of gas-phase ozone (36000 cm s^{-1} for O_3 at 296 K), r is the internal radius of the flow tube (r = 0.45 cm), k_{2nd} is the second-order rate constant of the aqueous-phase reaction between ACS and O_3, [ACS] is the concentration of ACS, and H_{O3} is the Henry's law constant of ozone in the dilute aqueous phase. The uptake coefficient of gas-phase ozone on an aqueous solution that contains ACS can be expressed from Eq-3, as follows:

$$\gamma = \frac{2rk_{1st}H_{O_3}RT}{\bar{v}} \quad \text{(Eq-4)}$$

If an aqueous solution contains salt ions, the Henry's law constant of ozone used for the dilute aqueous phase should be adjusted by the Setchenow equation that accounts for the effect of ionic

strength.[34,39] The used Henry's law constants of ozone at different salt concentrations are reported in Table S1.

3 Results and Discussion

3.1 Effect of O_3 concentration

The dependence of the reactive uptake coefficients on different ozone concentrations is reported in Figure 1. Figure 1 shows that the uptake coefficients decreased significantly (by a factor of 4), from $\gamma = (1.5 \pm 0.1)\times10^{-6}$ to $\gamma = (4.2 \pm 0.1)\times10^{-7}$, when increasing the O_3 concentrations from 2.46×10^{12} (100 ppb) to 2.46×10^{13} molecules cm^{-3} (1 ppm).

A saturation of the uptake coefficients was observed for ozone concentrations between 1.23×10^{13} and 2.46×10^{13} molecules cm^{-3}, which might be explained by fewer available adsorption sites on the liquid film. Hence, at high $[O_3]$ the ozone molecules that collide with the aqueous solution will have lower probability to adsorb and react at the surface.

This behavior of the uptake coefficients on the gas-phase concentrations of ozone is consistent with already reported studies[10,11,15,40,41] and implies a surface-mediated, Langmuir – Hinshelwood type uptake mechanism. This means that adsorption of the gas-phase oxidant would be followed by reaction at the liquid surface and possibly also in the bulk.[17-21,38]

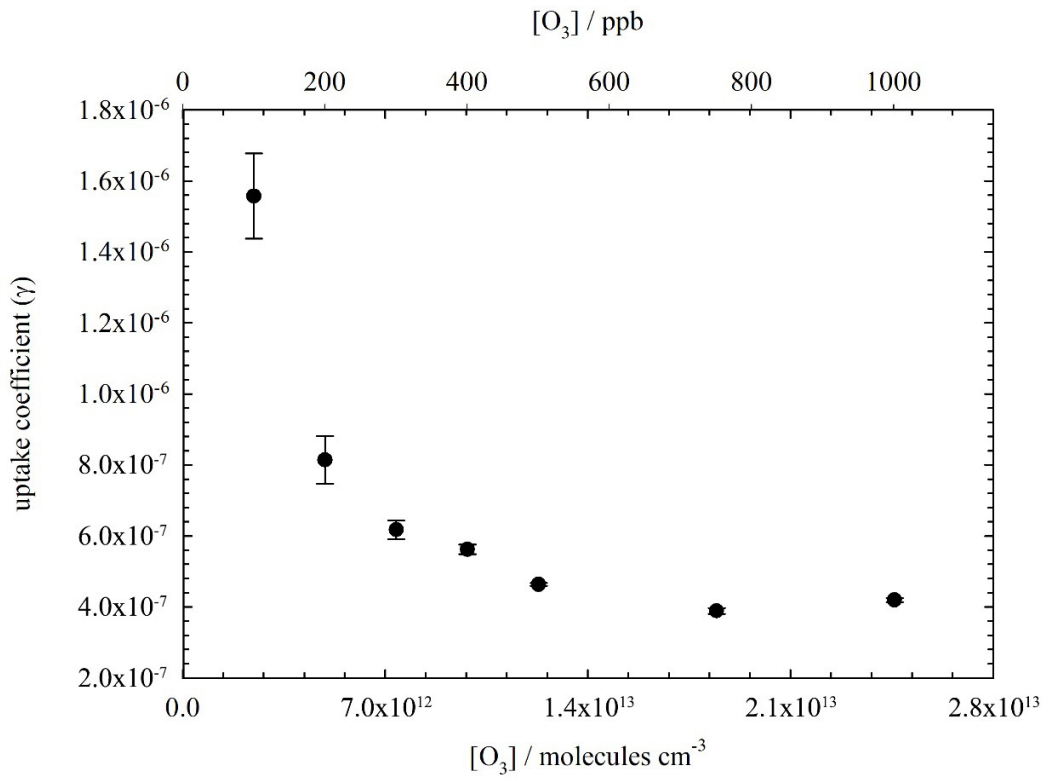

Figure 1: Reactive uptake coefficients of O_3 on aqueous solution of ACS (1×10^{-6} mol L^{-1}) *versus* different O_3 concentrations, in the presence of 0.05 mol L^{-1} of Na_2SO_4 at non-adjusted pH 8.85 and T = 296 K.

When kinetics is not influenced by mass accommodation, the corresponding uptake coefficients for surface reactions could be expressed in the following form, as suggested by Ammann et al. (2003):[21]

$$\frac{1}{\gamma} = \bar{v}\sigma\frac{1+K[O_s]_g}{4Kk_{1st}} \qquad \text{(Eq-5)}$$

Where $\bar{v}$ is the mean thermal velocity for ozone in the gas phase, σ is the surface area, taken up by a single adsorbed molecule of ozone, and K is the Langmuir adsorption equilibrium constant

of ozone. At high ozone concentrations, it can be assumed that $1 + K[O_3]_g \approx [O_3]_g$ and Eq-5 gets modified as follows:

$$\frac{1}{\gamma} \approx \frac{\bar{v}\sigma K}{4Kk_{1st}}[O_3]_g = \frac{\bar{v}\sigma}{4k_{1st}}[O_3]_g \quad \text{(Eq-6)}$$

To confirm that the kinetics is actually Langmuir-Hinshelwood like, Eq-5 was transformed into the following form:[40]

$$\frac{1}{\gamma} = \frac{\bar{v}\sigma}{4Kk_{1st}} + \frac{\bar{v}\sigma K}{4Kk_{1st}}[O_3]_g = A + AK[O_3]_g \quad \text{(Eq-7)}$$

A Langmuir-Hinshelwood kinetic mechanism could thus be confirmed as the data in Figure 2 follow linear regression:

$$\frac{1}{\gamma} = (8.8 \pm 0.2) \cdot 10^5 + (7.8 \pm 1.8) \cdot 10^{-8}[O_3] \,/\, molecules\ cm^{-3} \quad \text{(Eq-8)}$$

From the slope = AK = 7.75×10^{-8} cm^3 $molecule^{-1}$ and intercept = A = 8.84×10^5, the Langmuir adsorption equilibrium constant for ozone, K, was estimated as 8.8×10^{-14} cm^3 $molecules^{-1}$. The obtained value of K is consistent with the observed literature values for the heterogeneous reactions between ozone and different organic compounds at the water surface.[20,34,40,42,43]

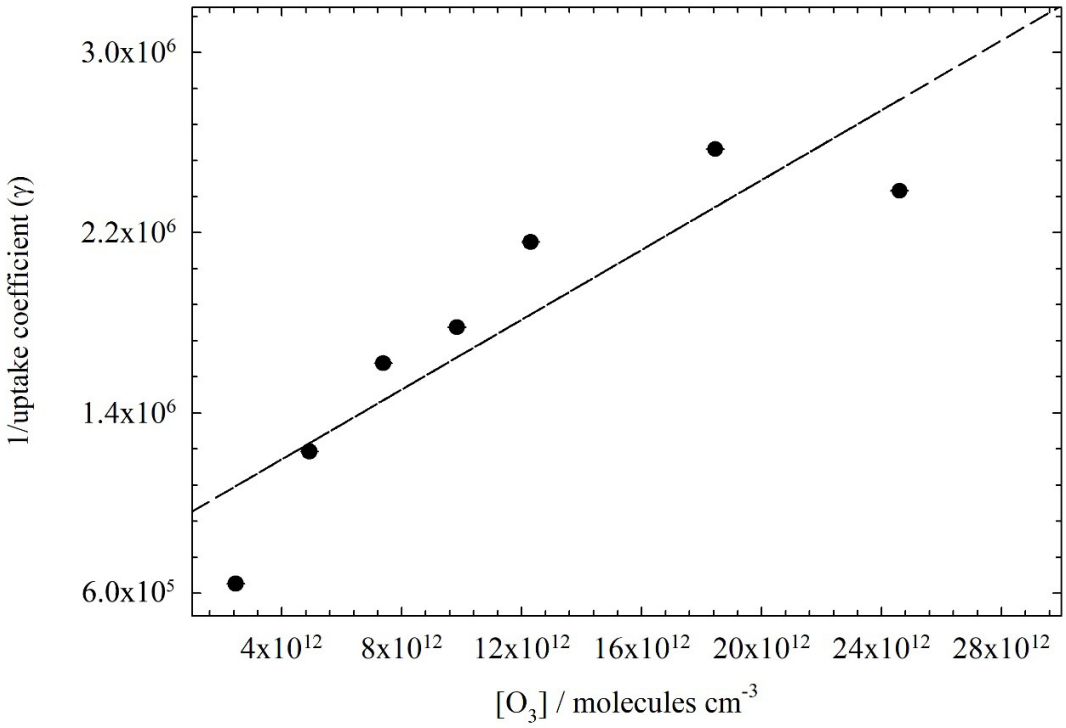

Figure 2: Reciprocal values of the reactive uptake coefficients of O_3 on a mixture of ACS (1×10^{-6} mol L^{-1}) and 0.05 mol L^{-1} of Na_2SO_4, versus different O_3 concentrations at non-adjusted pH 8.85 and T = 296 K.

3.2 Effect of ionic strength

The ionic strength can alter the kinetics and products distribution of reactions that occur within the aerosol deliquescent particles and, thus, can affect the aerosol composition and optical properties.[34,40,43-46]

It can be seen from Figure S2 that in the absence of ACS, the uptake coefficients are very low (close to the detection limit), and that they increase by 4 times, from $\gamma = (1.3 \pm 0.1)\times10^{-8}$ at $[SO_4^{2-}] = 0.05$ mol L^{-1} (I = 0.15 mol L^{-1}), to $\gamma = (5.1 \pm 0.8)\times10^{-8}$ for $[SO_4^{2-}] = 0.3$ mol L^{-1} (I = 0.9 mol L^{-1}). These results confirm that in the absence of organics, ozone reactions with aqueous

electrolytes solutions are extremely slow.[47] The uptake coefficient of O_3 on aqueous ACS at pH 5.76, in the absence of salt, is one order of magnitude higher compared to the uptake coefficient on neat salt solution (Figure S2).

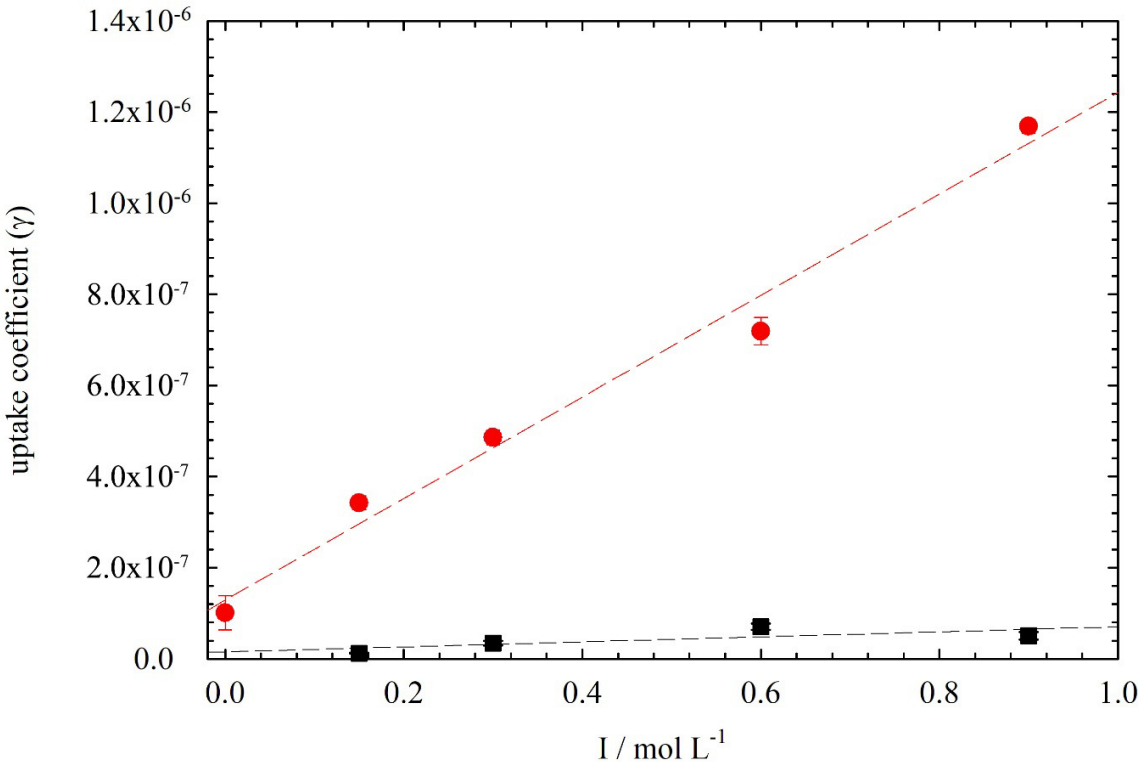

Figure 3: Uptake coefficients of ozone (300 ppb) as a function of molar ionic strength I. ■) Neat salt solution; ●) ACS, [ACS] = 1×10^{-6} mol L^{-1}, at pH = 3 by HCl. The error bars represent 2σ, resulting from the statistical error on the slope, which represents the first-order rate constant, k_{1st}. The long-dashed lines illustrate the linear regression for the uptake coefficients on a neat salt solution and in the presence of ACS.

Adding the salt ($[Na_2SO_4]$ = 0.05 mol L^{-1}) to an aqueous solution that initially contained ACS, increased the uptake of O_3 to $\gamma = (6.2 \pm 0.3)\times10^{-7}$. A further increase of salt concentration up to 0.3 mol L^{-1} (I = 0.9 mol L^{-1}) did not affect the uptake coefficients significantly (Figure S2). However, adding the salt alters the properties of the aqueous solution by decreasing the dielectric

constant of water (Table S1). As a consequence, the salt reduces the polarity of water that in turn affects the properties of ACS. The pH of the solution varied from 9.81 to 10.11 for a range of salt concentrations between 0.05 mol L^{-1} and 0.3 mol L^{-1}. The pKa value of ACS, which is (7.8 ± 0.2),[48] is thus influenced by the variation of ionic strength that affects the acid-base equilibrium and, hence, modifies the protonation/deprotonation fraction of ACS.[45] Consequently, the pH of the aqueous solution containing ACS was fixed to 3, which is typical for the acidic aerosols,[49] by addition of a proper volume of 1 mol L^{-1} HCl to investigate the effect of ionic strength alone on the uptake coefficients of ozone. At pH 3, a sharp increase was observed for the uptake coefficients of O_3 on aqueous ACS, from $\gamma = (1.4 \pm 0.4)\times10^{-7}$ in the absence of salt to $\gamma = (1.2 \pm 0.01)\times10^{-6}$ at $[Na_2SO_4]$ = 0.3 mol L^{-1} (Figure 3). The uptake coefficients of ozone, on an aqueous solution containing a mixture of ACS and SO_4^{2-} ions, are one to two orders of magnitude higher compared to the O_3 uptakes on a neat salt solution (Na_2SO_4). It has to be noted that the mean activity coefficient of the charged species present in the liquid phase decreases as the ion charge increases, and the hydrated ionic radius becomes smaller as the ionic strength of the liquid water increases. It has been shown that in concentrated aqueous solutions of inorganic salts, the large polarizable anions are enriched at the air-water interface compared to the small nonpolarizable cations.[50] Considering that the reaction of O_3 on neat SO_4^{2-} is not responsible for an increased ozone loss rate, it could be assumed that the presence of salt in aqueous solution could decrease the solubility of ACS due to the salting-out effect.[34,51] The salting-out effect implies an increase in the activity coefficient of ACS by dissolved Na_2SO_4, as has been previously observed for many non-polar organic compounds in concentrated electrolyte solutions.[52,53] In that case, the hydrogen-bonded OH groups of water would be displaced by the hydration shells of salt complexes,[53,54] and the increasing concentration of salt would result in

less available volume of the aqueous solution to dissolve ACS. The outcome is that ACS would be repelled towards the water-air interface and, as a consequence, the surface concentration of ACS would be higher in aqueous salt solutions compared to dilute aqueous phases, which increases the ozone loss rate at the surface.[34,41,54] Indeed, it has been demonstrated that the salting-out effect from the bulk aqueous phase is the controlling factor for the enrichment of organic compounds at the air-water interface.[55,56] Another possibility, also resulting in enhanced kinetics, could be interpreted in terms of the presence of ionic materials that influence the structure of water at the interface through an electric double layer, causing subsurface anions to approach closer to the air-liquid interface than cations.[57-59]

3.3 Influence of pH

The effect of pH on the uptake coefficients of O_3 was also investigated in the absence of salt. Actually, the reactivity of lignin-based compounds like ACS is strongly affected by the acidity of the phenolic functional group.[45,48] By comparing the uptake coefficients at different pH levels as reported in Figure 4, lower values of γ_{O3} were observed in the acidic range compared to neutral conditions.

Under alkaline conditions, the uptake of ozone increased even more, reaching a plateau at pH=10, $\gamma = (9.8 \pm 0.2)\times10^{-7}$, which is one order of magnitude higher than the uptake coefficient observed under acidic conditions ($\gamma = (8.8 \pm 0.8)\times10^{-8}$). At lower pH levels, phenolic compounds only occur in their protonated (neutral) form as a result of the large H^+ excess.

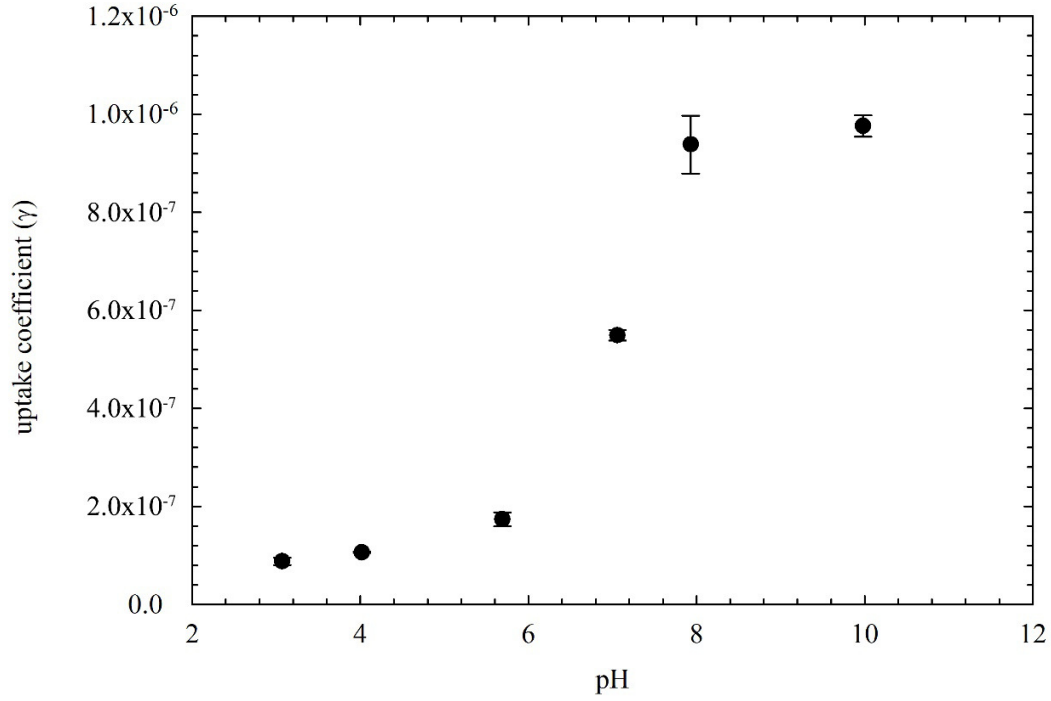

Figure 4: Uptake coefficients of O_3 (500 ppb) as a function of pH. The error bars represent 2σ, resulting from the statistical error on the slope, which represents the first-order rate constant, k_{1st}.

In these conditions, weak Van der Waals forces between neutral ACS and the surrounding H_2O/H_3O^+ species cause a structural variability and flexibility of ACS itself.[60] Moreover, the dynamic decomposition of phenols in a reaction with ozone can be more efficient and faster at pH ≥ 7.0.[61] At higher pH values, the phenolic group of ACS is ionized and the charge increment causes electrostatic repulsion, making the molecule to expand.[60] The reactivity of phenols with ozone increases at higher pH because the $–O^-$ group is a stronger activating group than the –OH group,[39] as observed experimentally (see Figure 4). The results shown in Figure 4 seem to be in good agreement with these findings, because increasing the pH leads to enhanced uptake coefficients as a consequence of the increasing occurrence of the more reactive deprotonated species.

Two possible pathways, which might occur between gas-phase ozone and ionized ACS molecules, are depicted in Scheme 1.

Scheme 1: proposed reaction mechanisms between ozone and ACS

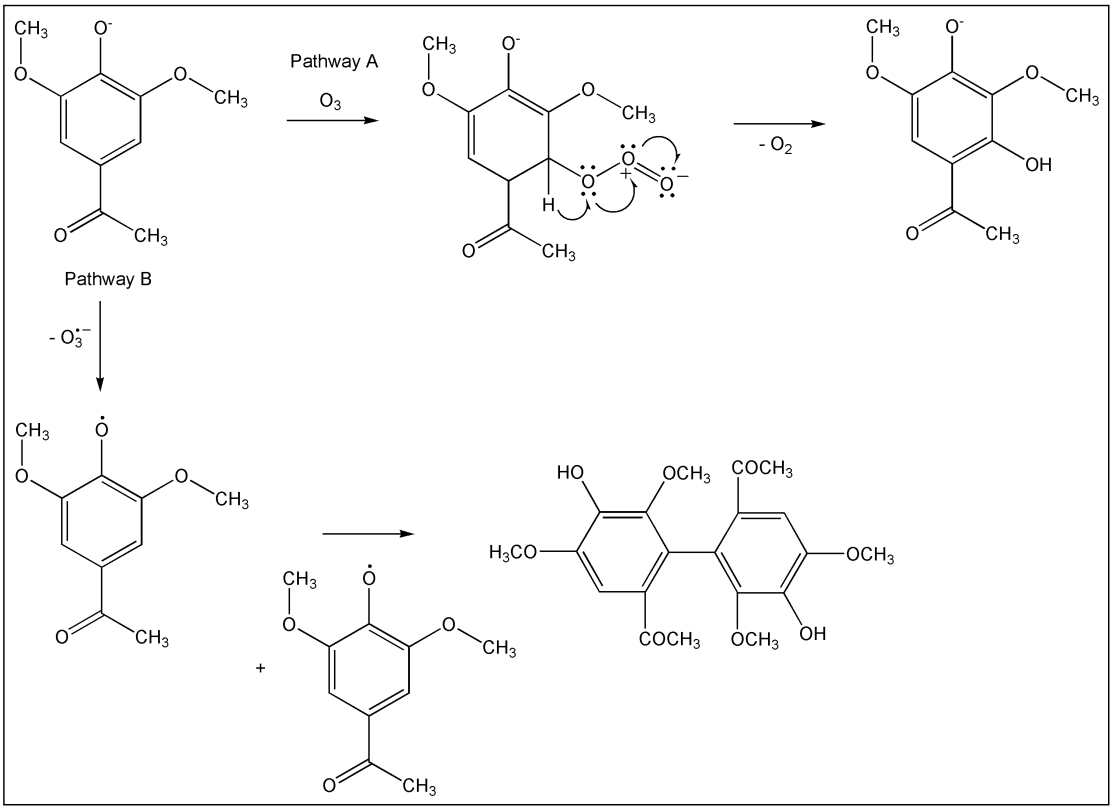

In the pathway A, it has been suggested the formation of ozone adducts. The hydroxylation of the aromatic ring would yield hydroxy phenolate (substituted resorcinol) after the release of oxygen. However, ozone might also oxidize the phenolate in order to form a phenoxy radical, which can easily dimerize (see Pathway B; here a dihydroxybiphenyl structure is shown as dimer, while phenoxyphenols are also possible reaction products).

3.4 Effect of temperature

The impact of temperature on the uptake coefficients of O_3 on ACS was investigated at five different temperature values, ranging from 278.15K to 318.15K. The uptake coefficients of O_3 on ACS measured in a dilute aqueous phase (representative of cloud droplets) and in the presence of 0.3 mol L^{-1} of Na_2SO_4 (representative of salt-rich aerosols) are plotted as a function of temperature in Figure S3. The uptake coefficients in dilute aqueous-phase are slightly enhanced, from $\gamma = (1.7 \pm 0.1)\times10^{-7}$ at 278.15K to $\gamma = (4.1 \pm 0.1)\times10^{-7}$ at 318.15K (see Figure S3). The obtained results seem to be consistent with those of a previous study focused on the heterogeneous reaction of O_3 with methoxyphenols.[15,62] The activation energy E_A of the heterogeneous reaction between O_3 and ACS was estimated by applying the Arrhenius law to the data reported in Figure 5.

The first-order rate constants of O_3 (k_{1st}) are related to the temperature T (K) as follows:

$$k_{1st} = \frac{\gamma \bar{c}}{2\, H_{Os}\, R\, T\, r} = A \exp\left(\frac{-E_A}{RT}\right) \quad \text{(Eq-9)}$$

where A is the pre-exponential factor and R is the gas constant (8.314 J mol^{-1} K^{-1}).

From the linear regressions of the plots depicted in Figure 5, the following equations are derived that correspond to a dilute aqueous-phase (Eq-10) and to I = 0.9 mol L^{-1} Na_2SO_4 (Eq-11):

$$k_{1st}(T) = (21.3 \pm 0.5) \exp\left(\frac{-1857.3 \pm 419.8}{T}\right) s^{-1} \quad \text{(Eq-10)}$$

$$k_{1st}(T) = (36.3 \pm 0.5) \exp\left(\frac{-2164.6 \pm 463.8}{T}\right) s^{-1} \quad \text{(Eq-11)}$$

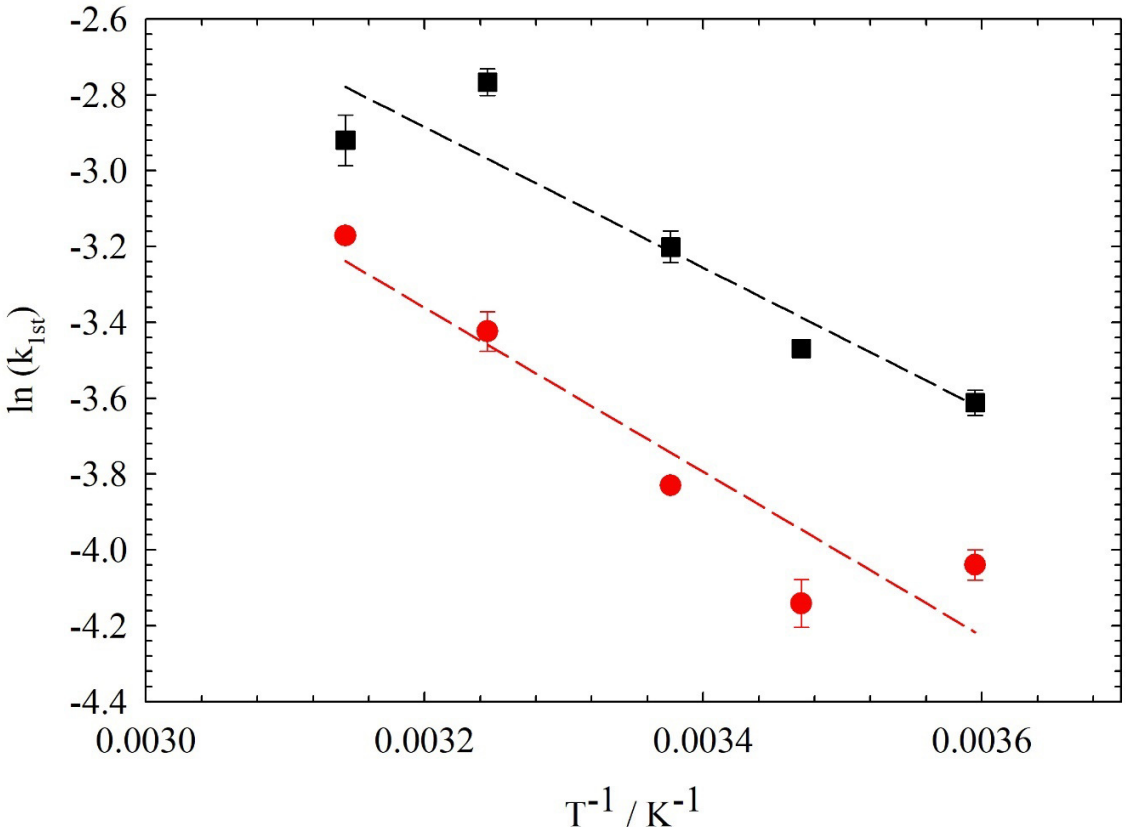

Figure 5: Temperature-dependent first-order rate constant (k_{1st}) of O_3 (300 ppb): ■) in the absence of salt, and ●) in the presence of 0.3M SO_4^{2-}. The errors bars represent 2σ, resulting from the statistical error on the slope.

The values of A and E_A are derived from the intercept and the slope of the regression lines, respectively. It is remarkable to observe a great similarity of the slope of the plot in the presence of sulfate ions, and in the dilute aqueous phase. Moreover, the activation energy for the reaction in the presence of 0.3 mol L^{-1} of Na_2SO_4 is comparable (E_A=18.0 kJ mol^{-1}) to that obtained in the absence of SO_4^{2-} ions (E_A=15.4 kJ mol^{-1}). This finding is consistent with the hypothesis that an increase in the ionic strength does not modify the energetics of the reaction, but it rather changes the availability of ACS at the water surface.

3.5 Modeling of the uptake coefficients

The experimental data reported in Figures 1, 3 and 4 suggest that the uptake coefficient γ has a significant dependence on [O_3], the ionic strength and the pH value of the aqueous solution. Moreover, Eqs. (2-4) suggest that γ is also directly proportional to [ACS]. These considerations suggest that it should be possible to derive a general fit equation that describes phenomenologically the trend of γ as a function of the different experimental parameters. Based on multiple data fits, the following equation is thus proposed:

$$\gamma = \frac{[ACS]}{0.725 + 0.011[O_3]} \times \frac{0.40 \times 10^{-pH} + 10^{-7.1}}{10^{-pH} + 10^{-7.1}} \times (1 + 34.3\, c_{Na_2SO_4}) \qquad \text{(Eq-12)}$$

where [ACS] and $c_{Na_2SO_4}$ are expressed in mol L^{-1} units, and [O_3] (gas phase) in ppb. Moreover, the ionic strength I = 3 $c_{Na_2SO_4}$, thus $c_{Na_2SO_4}$ = ⅓ I. The ability of Eq-12 to predict the experimental values of γ *vs.* [O_3] and γ *vs.* $c_{Na_2SO_4}$, obtained at different pH values, is reported in Figure S4. Interestingly, the effect of pH described by Eq-12 is suitable to fit the experimental data of γ obtained in the presence of a background electrolyte at different pH values, but the pH trend described by this equation is less marked than the pH effect observed in the absence of salt. The most likely reason is that added electrolyte, such as Na_2SO_4, has a salting-out effect on neutral (undissociated) ACS and increases its concentration at the air-water interface, thereby enhancing the reaction with O_3. In contrast, no such effect is observed with anionic (basic) ACS (the phenolate form). Therefore, the reactivity difference between neutral and anionic ACS is less marked in the presence of added salt than in its absence.

The phenomenological Eq-12 can be used to assess the behaviour of γ under reasonable environmental conditions (see Figure 6), included within the experimental ranges where the equation was derived (phenomenological equations allow interpolations, not extrapolations). In particular, the value of O_3 was here varied from pristine atmosphere to moderately high pollution conditions (up to 200 ppb), and the pH range (3-7) is reasonable for atmospheric aerosols.[49]

More acidic conditions (pH < 3) would also be atmospherically relevant, but they were not investigated because Eq-12 does not allow extrapolation beyond the experimental conditions in which it was obtained. A similar issue holds for the ionic strength that can reach values > 0.9 mol L^{-1}, which is the upper limit of the experimentally investigated range. Finally, the linear dependence of γ *vs.* [ACS] is accounted for by the pseudo-first order trend of $[O_3]$ *vs. t*. (Eqs. 2-4).

The trends reported in Figure 6 obviously suggest that the uptake coefficient γ would be significantly affected by the occurrence of ACS. However, the effect of ACS on γ would be most marked at low $[O_3]$ and high I. The effect would also be somewhat higher at high compared to low pH, but in this case the predicted differences with varying pH are not as high as for the other parameters, and they are really limited at pH < 6.

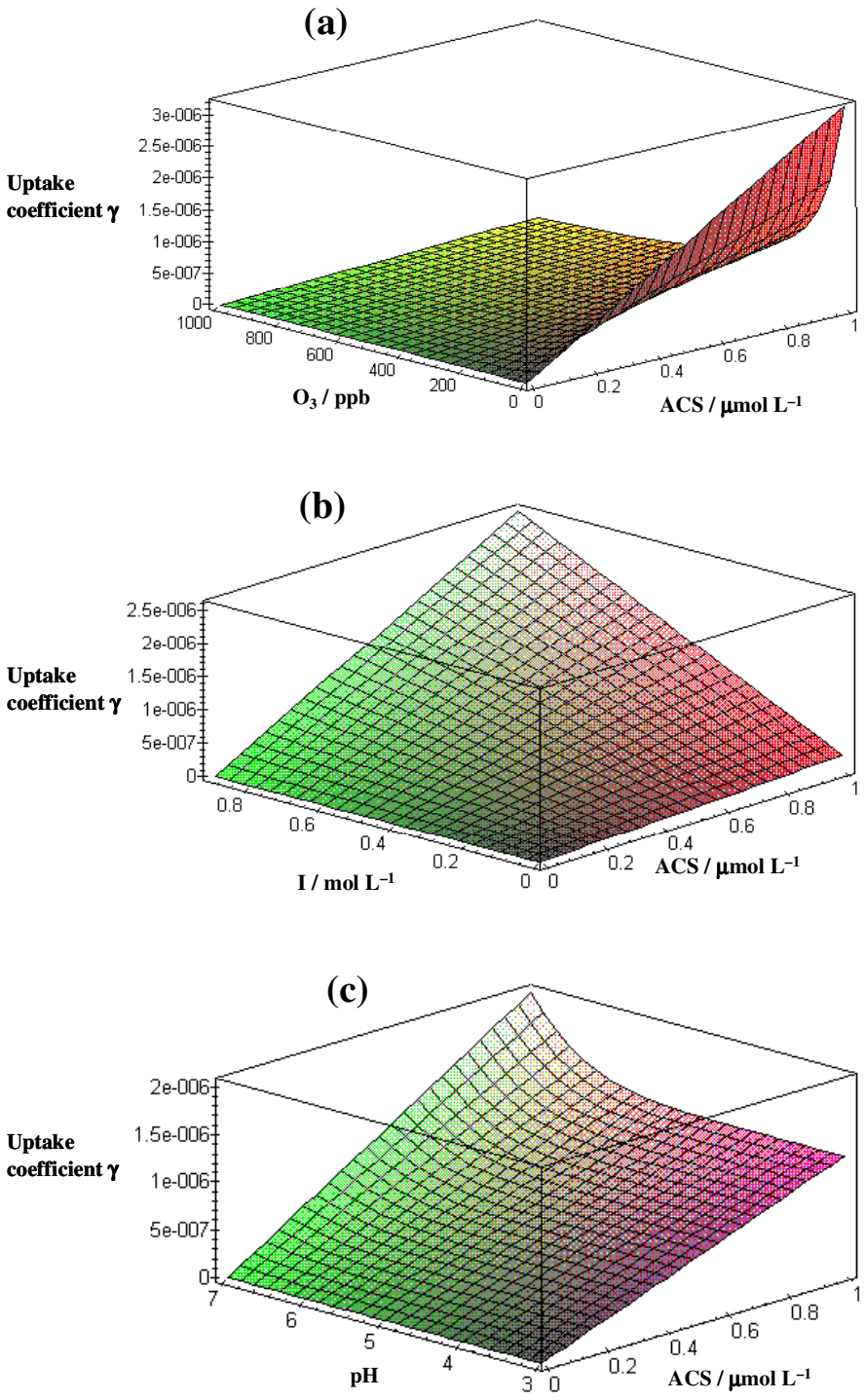

Figure 6: Predicted trends of the uptake coefficient γ, as a function of the studied experimental parameters under environmentally significant conditions. **(a)** γ *vs.* [O_3] and [ACS]; **(b)** γ *vs.* I (ionic strength) and [ACS]; **(c)** γ *vs.* pH and [ACS]. When not varying, the parameters were set as follows: [O_3] = 100 ppb, I = 0.4 mol L^{-1}, pH 5.5.

3.6 Atmospheric implications

We investigated the heterogeneous reactions occurring between gas-phase ozone and an aqueous-phase solution of a lignin model compound (ACS), with and without SO_4^{2-} ions. Moreover, first-order reaction rate constants were determined as a function of ozone concentrations, pH values and temperature, with a focus on the effect of the ionic strength on the heterogeneous oxidation kinetics. At pH 3, which is typical for acidic aerosol particles, the uptake of ozone on ACS exhibited a sharp linear relationship with the ionic strength, which resulted into one to two orders of magnitude faster kinetics compared to the ozone uptakes on a neat salt solution containing only SO_4^{2-} ions. These results highlight the importance of the ionic strength effect and suggest a much faster oxidation kinetics of methoxyphenols in aerosol deliquescent particles, compared to that in the dilute aqueous phase of cloud droplets. An obvious factor strongly affecting the uptake coefficients of ozone on ACS, and potentially on other methoxyphenols, is the pH of the aqueous solution. Indeed, we observed one order of magnitude faster heterogeneous oxidation in alkaline media compared to acidic conditions. The effective uptake of ozone by an aqueous solution, containing ACS mixed with elevated concentrations of SO_4^{2-} ions, suggests that methoxyphenols might have a significant potential to contribute to the consumption of ozone in the troposphere.

The importance of different atmospheric gas-phase oxidants in the heterogeneous oxidation of surface-bound lignin model compounds, could be more relevantly assessed by using the oxidative power than by considering the uptake coefficients. The oxidative power is commonly referred to as the product between the uptake coefficient of the gas-phase oxidant times its concentration ($\gamma_{O3} \times [O_3]_g$).[63] A higher value of oxidative power implies a more important removal

process of the organic compounds.[63] Table 1 describes the calculated values of the oxidative power of ozone, and its comparison with previous studies.[19]

Table 1 shows that the oxidative power of ozone is enhanced by one order of magnitude at elevated ionic strength, compared to a dilute aqueous phase. Considering the high concentrations of inorganic salts occurring in aerosol deliquescent particles during haze events, the oxidative powers of different atmospheric oxidants (certainly ozone, but possibly also OH) might become considerably higher than those predicted for oxidation reactions in cloud droplets. Indeed, if the ionic-strength effect is due to higher occurrence of ACS (and, presumably, other phenolic compounds as well) at the water-air interface, an acceleration of the reaction kinetics would be observed in the presence of all the gas-phase oxidants.

Table 1: Comparison of the oxidative power of ozone and OH towards lignin-based compounds

substrate	$\gamma_{O3}\times[O_3]$[a]	Reference
ACS	3.4×10^5	This study
ACS + 0.3M SO_4^{2-}	3.0×10^6	This study
Levoglucosan	3.3×10^7	Knopf et al. (2011)[19]
Abietic acid	1.4×10^8	Knopf et al. (2011)[19]
Nitroguaiacol	2.0×10^8	Knopf et al. (2011)[19]
Mixture of levoglucosan, abietic acid and nitroguaiacol	1.7×10^8	Knopf et al. (2011)[19]

[a] concentration of O_3 and OH are used for typical atmospheric values of polluted environment like 100 ppb and 0.04ppt, respectively.[1]

[b] $\gamma_{OH}[OH] = 1.0\times10^6$.[19,64]

Based on the obtained first-order rate constants, the atmospheric lifetime of the investigated lignin surrogates due to the gas-phase oxidation with ozone was calculated according to the following equation:[19,63]

$$\tau = \frac{4N_{tot}}{\gamma \bar{v}[ox]_g} \quad \text{(Eq-13)}$$

Where N_{tot} denotes the surface concentration of the organic molecules (molecules cm^{-2}), $\bar{v}$ is the mean thermal velocity (cm s^{-1}), and $[ox]_g$ is the concentration of the gas-phase oxidant (molecules cm^{-3}). Here, it was assumed $N_{tot} = 10^{14}$ cm^{-2}.[19,63,65] Taking into account the average ozone concentration (7.38×10^{14} molecules cm^{-3}), atmospheric lifetimes of surface-bound ACS and of a mixture of ACS and 0.3 mol L^{-1} SO_4^{2-} at pH = 3 were calculated as 2.48 min and 12.9 s, respectively, due to the nighttime heterogeneous reactions with ozone in cloud droplets and aerosol deliquescent particles. The obtained atmospheric lifetime of ACS is comparable with the lifetimes of other methoxyphenols.[15,19,66] These results undoubtedly indicate that methoxyphenols have an ability to get more easily oxidized through heterogeneous processes in atmospheric aerosol deliquescent particles, compared to the aqueous phase reactions in clouds.

It has to be noted that the nature of the electrolytes present in the liquid water of aerosol particles may play an important role on the uptake coefficients of ozone and other atmospheric oxidants. Therefore, the treatment of the heterogeneous oxidation reactions in atmospheric models describing the aerosol chemistry, without considering the ionic strength effect on the reaction rates, would introduce errors and lead to incorrect outcomes. Only by considering the ionic strength effects the models can correctly describe the absorption or scattering properties of aerosol particles and cloud droplets, which is of the utmost importance to enable accurate estimates of the radiative forcing of clouds and aerosols.

Associated content

Acknowledgment

This study was financially supported by the Chinese Academy of Science, International Cooperation Grant (N°: 132744KYSB20190007) and National Natural Science Foundation of China (N°: 41773131, and N°: 41977187).

Supporting Information

Additional 1 table and 4 figures. The supporting information is available free of charge via the Internet on the ACS Publications website at http://pubs.acs.org.

Author information

Corresponding Author

* Phone: +86 2085291497; Email: gligorovski@gig.ac.cn

Notes

The authors declare no competing financial interest.

References

1. Finlayson-Pitts, B. J.; Pitts, Jr., J. N. *Chemistry of the Upper and Lower Atmosphere, Theory, Experiments, and Applications*; Academic Press: California, U. S. A., 2000.

2. Marufu, L.; Dentener, F.; Lelieveld, J.; Andreae, M. O.; Helas, M. Photochemistry of the African troposphere: Influence of biomass-burning emissions. *J. Geophys. Res*. **2000**, *105*, 14513-14530.

3. Chen, J.; Li, C.; Ristovski, Z.; Milic, A.; Gu, Y.; Islam, M. S.; Wang, S.; Hao, J.; Zhang, H.; He, C.; Guo, H.; Fu, H.; Miljevic, B.; Morawska, L.; Thai, P.; Lam, Y. F.; Pereira, G.; Ding, A.; Huang, X.; Dumka, U. C. A review of biomass burning: Emissions and impacts on air quality, health and climate in China. *J. Sci. Toten*. **2017**, *579*, 1000-1034.

4. Tan, K. H.; *Humic Matter in Soil and the Environment Principles and Controversies*; CRC Press: Florida, U.S.A., 2014.

5. Mazzoleni, L. R.; Zielinska, B.; Moosmueller, H. Emissions of Levoglucosan, Methoxy Phenols, and Organic Acids from Prescribed Burns, Laboratory Combustion of Wildland Fuels, and Residental Wood Combustion. *Environ. Sci. Technol.* **2007**, *41*, 2115-2122.

6. Vione, D.; Maurino, V.; Minero, C.; Pelizzetti, E.; Harrison, M. A. J.; Olariu, R.-I.; Arsene, C. Photochemical reaction in the tropospheric aqueous phase and on matriculate matter. *Chem. Soc. Rev*. **2006**, *35*, 441-453.

7. Simoneit, B. R. T. Biomass burning — a review of organic tracers for smoke from incomplete combustion. Applied Geochem. **2002**, *17*, 129–162.

8. Cuisset, A.; Coeur, C.; Mouret, G.; Ahmad, W.; Tomas, A.; Pirali, O. Infrared spectroscopy of methoxyphenols involved as atmospheric secondary organic aerosol precursos: gas-phase vibrational cross-sections. *J. Quant. Spectrosc. Radiat. Transf.* **2016**, *179*, 51–58.

9. Schauer, J. J.; Kleeman, M. J.; Cass, G. R.; Simoneit, B. R. T. Measurement of Emissions from Air Pollution Sources. 3. C1-C29 Organic Compounds from Fireplace Combustion of Wood. *Environ. Sci. Technol*. **2001**, *35*, 1716-1728.

10. Net, S.; Nieto-Gligorovski, L.; Gligorovski, S.; Wortham, H. Heterogeneous ozonation kinetics of 4-phenoxyphenol in the presence of photosensitizer. *Atmos. Chem. Phys*. **2010**, *10*, 1545–1554.

11. Net, S.; Gligorovski, S.; Pietri, S.; Wortham, H.: Photoenhanced degradation of veratraldehyde upon the heterogeneous ozone reactions. *Phys. Chem. Chem. Phys*. **2010**, *12*, 7603-7611.

12. El Zein, A.; Coeur, C.; Obeid, E.; Lauraguais, A.; Fagniez, T. Reaction Kinetics of Catechol (1,2-Benzenediol) and Guaiacol (2-Methoxyphenol) with Ozone. *J. Phys. Chem. A* **2015**, *119*, 6759-6765.

13. Sun, Y.; Xub, F.; Lia, X.; Zhang, Q.; Gu, Y. Mechanisms and Kinetic Studies of OH-initiated Atmospheric Oxidation of Methoxyphenols in the Presence of O_2 and NOx. *Phys. Chem. Chem. Phys.* **2019**, *21*, 21856-21866.

14. Jammoul, A.; Gligorovski, S.; George, C.; D'Anna, B. Photosensitized Heterogeneous Chemistry of Ozone on Organic Films. *J. Phys. Chem. A* **2008**, *112*, 1268-1276.

15. Zhang, T.; Yang, W.; Han, C.; Yang, H.; Xue, X. Heterogeneous reaction of ozone with syringic acid: Uptake of O_3 and changes in the composition and optical property of syringic acid. *Environ. Poll.* **2020**, *257*, 113632.

16. He, L.; Schaefer, T.; Otto, T.; Kroflič, A.; Herrmann, H. Kinetic and Theoretical Study of the Atmospheric Aqueous-Phase Reactions of OH Radicals with Methoxyphenolic Compounds. *J. Phys. Chem. A* **2019**, *123*, 7828−7838.

17. Ammann, M; Rössler, E.; Strekowski, R.; George, C. Nitrogen dioxide multiphase chemistry: Uptake kinetics on aqueous solutions containing phenolic compounds. *Phys. Chem. Chem. Phys.* **2005**, 7, 2513–2518.

18. Shiraiwa, M.; Poschl, U.; Knopf, D. A. Multiphase chemical kinetics of NO_3 radicals reacting with organic aerosol components from biomass burning. *Environ. Sci. Technol.* **2012**, *46*, 6630– 6636.

19. Knopf, D. A.; Forrester, S. M.; Slade, J. H. Heterogeneous oxidation kinetics of organic biomass burning aerosol surrogates by O_3, NO_2, N_2O_5, and NO_3. *Phys. Chem. Chem. Phys.* **2011**, *13*, 21050–21062.

20. Forrester, S. M.; Knopf, D. A. Photosensitised heterogeneous oxidation kinetics of biomass burning aerosol surrogates by ozone using an irradiated rectangular channel flow reactor. *Atmos. Chem. Phys.* **2013**, *13* (13), 6507–6522.

21. Ammann, M.; Poeschl, U.; Rudich, Y. Effects of reversible adsorption and Langmuir–Hinshelwood surface reactions on gas uptake by atmospheric particle. *Phys. Chem. Chem. Phys.* **2003**, *5*, 351–356.

22. Yee, L. D.; Kautzman, K. E.; Loza, C. L.; Schilling, K. A.; Coggon, M. M.; Chhabra, P. S.; Chan, M. N.; Chan, A. W. H.; Hersey, S. P.; Crounse, J. D.; Wennberg, P. O.; Flagan, R. C.; Seinfeld, J. H. Secondary organic aerosol formation from biomass burning intermediates: phenol and methoxyphenols. *Atmos. Chem. Phys.* **2013**, *13*, 8019–8043.

23. Lauraguais, A.; Coeur-Tourneur, C.; Cassez, A.; Deboudt, K.; Fourmentin, M.; Choel, M. Atmospheric reactivity of hydroxyl radicals with guaiacol (2-methoxyphenol), a biomass burning emitted compound: Secondary organic aerosol formation and gas-phase oxidation products. *Atmos. Environ.* **2014**, *86*, 155-163.

24. Liu, C.; Liu, Y.; Chen, T.; Liu, J.; He, H. Secondary organic aerosol formation from the OH-initiated oxidation of guaiacol under different experimental conditions. *Atmos. Environ.* **2019**, *207*, 30-37.

25. Sicard, P.; Serra, R.; Rossello, P. Spatiotemporal trends in ground-level ozone concentrations and metrics in France over the time period 1999–2012. *Environ. Res.* **2016**, *149*, 122-144.

26. Lee, Y. C.; Shindell, D. T.; Faluvegi, G.; Wenig, M. Lam, Y. F.; Ning, Z.; Hao, S.; Lai, C. S. Increase of ozone concentrations, its temperature sensitivity and the precursor factor in South China. *Tellus B Chem Phys Meteorol.* **2014**, *66*, 23455.

27. Wang, T.; Dai, J.; Lam, K. S; Nan Poon, C.; Brasseur, G. P. Twenty - Five Years of Lower Tropospheric Ozone Observations in Tropical East Asia: The Influence of Emissions and Weather Patterns. *Geophys. Res. Lett.* **2019**, *46*, 11463-11470.

28. Yang, G.; Liu, Y.; Li, X. Spatiotemporal distribution of ground-level ozone in China at a city level. Sci. Rep. 2020, 10 (7229), 1-12.

29. Lu, X.; Zhang, L.; Wang, X.; Gao, M.; Li, K.; Zhang, Y.; Yue, X.; Zhang, Y. Rapid Increases in Warm-Season Surface Ozone and Resulting Health Impact in China Since 2013. *Environ. Sci. Technol. Lett.* **2020**, *7* (4), 240-247.

30. Zhang, J.; Wei, Y.; Fang, Z. Ozone Pollution: A Major Health Hazard Worldwide. *Front. Immunol.* **2019**, *10* (2518), 1-10.

31. Herrmann, H. Kinetics of Aqueous Phase Reactions Relevant for Atmospheric Chemistry. *Chem. Rev.* **2003**, *103*, 4691−4716.

32. Herrmann, H.; Schaefer, T.; Tilgner, A.; Styler, S. A.; Weller, C.; Teich, M.; Otto, T. Tropospheric Aqueous-Phase Chemistry: Kinetics, Mechanisms, and Its Coupling to a Changing Gas Phase. *Chem. Rev.* **2015**, *115*, 4259−4334.

33. Cheng, Y.; Zheng, G.; Wei, C.; Mu, Q.; Zheng, B.; Wang, Z.; Gao, M.; Zhang, Q.; He, K.; Carmichael, G.; Pöschl, U.; Su, H. Reactive nitrogen chemistry in aerosol water as a source of sulfate during haze events in China. *Sci. Adv.*, **2016**, *2*, 1-11.

34. Mekic, M.; Loisel, G.; Zhou, W.; Jiang, B.; Vione, D.; Gligorovski, S. Ionic strength effects on the reactive uptake of ozone on aqueous pyruvic acid: Implications for air-sea ozone deposition. *Environ. Sci. Technol.* **2018**, *52* (21), 12306-12315.

35. Huthwelker, T.; Ammann, M.; Peter, T. The uptake of acidic gases on ice. *Chem. Rev.* **2006**, *106*, 1375-1444.

36. Behnke, W.; George, C.; Scheer, V. Zetzsch, C. Production and decay of ClNO2 from the reaction of gaseous N_2O_5 with NaCl solution: bulk and aerosol experiments. *J. Geophys. Res.* **1997**, *102*, 3795-3804.

37. Barcellos da Rosa, M.; Behnke, W.; Zetzsch, C. Study of the heterogeneous reaction of O_3 with CH_3SCH_3 using the wetted-wall flowtube technique. *Atmos. Chem. Phys*. **2003**, *3*, 1665–1673.

38. Gutzwiller, L.; George, C.; Roessler, E.; Ammann, M. Reaction Kinetics of NO_2 with Resorcinol and 2,7-Naphthalenediol in the Aqueous Phase at Different pH. *J. Phys. Chem. A* **2002**, *106*, 12045-12050.

39. Beltran, F. J. *Ozone reaction kinetics for water and wastewater systems*; CRC Press LLC: 686 Florida, U. S. A., 2004.

40. Oldridge, N. W.; Abbatt, J. P. D. Formation of Gas-Phase Bromine from Interaction of Ozone with Frozen and Liquid NaCl/NaBr Solutions: Quantitative Separation of Surficial Chemistry from Bulk-Phase Reaction. *J. Phys. Chem. A* **2011**, *115*, 2590–2598.

41. Clifford, D.; Donaldson, D. J.; Brigante, M.; D'Anna, B.; George, C. Reactive Uptake of Ozone by Chlorophyll at Aqueous Surfaces. *Environ. Sci. Technol*. **2008**, *42*, 1138–1143.

42. Mmereki, B. T.; Donaldson, D. J. Direct observation of the kinetics of an atmospherically important reaction at the air−aqueous interface. *J. Phys. Chem. A* **2003**, *107*, 11038-11042.

43. Reeser, D. I.; Jammoul, A.; Clifford, D.; Brigante, M.; D'Anna, B.; George, C.; Donaldson, D. J. Photoenhanced Reaction of Ozone with Chlorophyll at the Seawater Surface. *J. Phys. Chem. C* **2009**, *113*, 2071–2077.

44. Mekic, M.; Brigante, M.; Vione, D.; Gligorovski, S. Exploring the ionic strength effects on the photochemical degradation of pyruvic acid in atmospheric deliquescent aerosol particles. *Atmos. Environ*. **2018**, *185*, 237-242.

45. Zhou, W.; Mekic, M.; Liu, J.; Loisel, G.; Jin, B.; Vione, D.; Gligorovski, S. Ionic strength effects on the photochemical degradation of acetosyringone in atmospheric deliquescent aerosol particles. *Atmos. Environ*. **2019**, *198*, 83-88.

46. Mekic, M.; Zeng, J.; Zhou, W.; Loisel, G.; Jin, B.; Li, X.; Vione, D.; Gligorovski, S. The ionic strength effect on photochemistry of fluorene and DMSO at the air-sea interface: Alternative formation pathway of organic sulfur compounds in marine atmosphere. *ACS Earth Space Chem*. **2020**, DOI: 10.1021/acsearthspacechem.0c00059.

47. Ershov, B. G.; Gordeev, A. V.; Seliverstov, A. F. Ozone Solubility in Aqueous Solutions of NaCl, Na_2SO_4, and K_2SO_4: Application of the Weisenberger-Schumpe Model for Description of Regularities and Calculation of the Ozone Molar Absorption Coefficient. *Ozone: Sci. Eng*. **2017**, *39*, 69-72.

48. Ragnar, M.; Lindgren, C. T.; Nilvebrant, N-O. pKa-Values of Guaiacyl and Syringyl Phenols Related to Lignin. *J. Wood Chem. Technol*. **2000**, *20*, 277-305.

49. Pye, H. O. T.; Nenes, A.; Alexander, B.; Ault, A. P.; Barth, M. C.; Clegg, S. L.; Collett Jr., J. L.; Fahey, K. M.; Hennigan, C. J.; Herrmann, H.; Kanakidou, M.; Kelly, J. T.; Ku,

I-T.; McNeill, V. F.; Riemer, N.; Schaefer, T.; Shi, G.; Tilgner, A.; Walker, J. T.; Wang, T.; Weber, R.; Xing, J.; Zaveri, R. A.; Zuend, A. The acidity of atmospheric particles and clouds. *Atmos. Chem. Phys*. **2020**, *20*, 4809–4888.

50. Knipping, E. M; Lakin, M. J.; Foster, K. L.; Jungwirth, P.; Tobias, D. J.; Gerber, R. B.; Dabdub, D.; Finlayson-Pitts, B. J. *Science*. **2000**, *288*, 301-304.

51. Endo, S.; Pfennigsdorff, A.; Goss, K.-U. Salting-out effect in aqueous NaCl solutions: trends with size and polarity of solute molecules. *Environ. Sci. Technol.* **2012**, *46*, 1496−1503.

52. Zuend, A.; Marcolli, C.; Luo, B. P.; Peter, T. A thermodynamic model of mixed organic-inorganic aerosols to predict activity coefficients. *Atmos. Chem. Phys*. **2008**, *8*, 4559–4593.

53. Panagopoulos, D.; Kierkegaard, A.; Jahnke, A.; MacLeod, M. Evaluating the Salting-Out Effect on the Organic Carbon/Water Partition Ratios (KOC and KDOC) on Linear and Cyclic Volatile Methylsiloxanes: Measuremnts and Polyparameter Linear Free Energy Relationships. *J. Chem. Eng. Data*. **2016**, *61*, 3098-3108.

54. Demou, E.; Donaldson, D. J. Adsorption of Atmospheric Gases at the Air-Water Interface. 4: The Influence of Salts. *Phys. Chem. A* **2002**, *106*, 982-987.

55. Soule, M. C. K.; Blower, P. G.; Richmond, G. L. Effects of Atmospherically Important Solvated Ions on Organic Acid Adsorption at the Surface of Aqueous Solutions. *J. Phys. Chem. B*. **2007**, *111* (49), 13703–13713.

56. Sahu, K.; McNeill, V. F.; Eisenthal, K. B. Effect of Salt on the Adsorption Affinity of an Aromatic Carbonyl Molecule to the Air-Aqueous Interface: Insight for Aqueous Environmental Interfaces. *J. Phys. Chem. C*. **2010**, *114*, 18258–18262.

57. Jungwirth, P.; Tobias, D. J. Specific Ion Effects at the Air/Water Interface. *Chem. Rev*. **2006**, *106*, 1259−1281.

58. Schnitzer, C.; Baldelli, S.; Shultz, M. J. Sum Frequency Generation of Water on NaCl, $NaNO_3$, $KHSO_4$, HCl, HNO_3, and H_2SO_4 Aqueous Solutions. *J. Phys. Chem. B* **2000**, *104*, 585-590.

59. Schutz, M. J.; Baldelli, S.; Schnitzer, C.; Simonelli, D. *Water Confined at the Liquid-Air Interface*; Springer: Heidelberg, Germany, 2003. (DOI: 10.1007/978-3-662-05231-0_12)

60. Alvarez-Puebla, R. A.; Valenzuela-Calahorro, C.; Garrido, J. J. Theoretical study on fulvic acid structure, conformation and aggregation A molecular modelling approach. *Sci. Total Environ*. **2006**, *358*, 243-254.

61. Poznyak, T.; Vivero, J. Degradation of Aqueous Phenol and Chlorinated Phenols by Ozone. *Ozone: Sci. Eng*. **2005**, *27*, 447-458.

62. Friebel, F.; Mensa, A. A. Ozone concentration versus Temperature: Atmospheric aging of soot particles. *Langmuir* **2019**, *35*, 14437-14450.

63. Gross, S.; Bertram, A. K. Reactive Uptake of NO_3, N_2O_5, NO_2, HNO_3, and O_3 on Three Types of Polycyclic Aromatic Hydrocarbon Surfaces. *J. Phys. Chem. A* **2008**, *112*, 3104-3113.

64. Kessler, S. H.; Smith, J. D.; Che, D. L.; Worsnop, D. R.; Wilson, K. R.; Kroll, J. H. OH-Initiated Heterogeneous Aging of Highly Oxidized Organic Aerosol. *Environ. Sci. Technol.* **2010**, *44*, 7005–7010.

65. Moise, T.; Rudich, Y. Uptake of C1 and Br by organic surfaces - a perspective on organic aerosols processing by tropospheric oxidants. *J. Geophys. Res. Lett*. **2001**, *28*, 4083-4086.

66. O'Neill, E. M.; Kawam, A. Z.; Van Ry, D. A.; Hinrichs, R. Z. Ozonolysis of surface-adsorbed methoxyphenols: kinetics of aromatic ring cleavage vs. alkene side-chain oxidation. *Atmos. Chem. Phys*. 2014, 14, 47–60.